Zero-bias error compensation method of laser gyro based on neural network

Juan Cui

Department of Basic Courses,
Xi'an Traffic Engineering Institute,
Xi'an, Shaanxi Province, China
Email: cj15353742809@126.com

Cong Zhong*

Technical Department,
Xi'an North Jierui Opto-electronic Technology Co., Ltd.,
Xi'an, Shaanxi Province, China
Email: 13720753899@163.com
*Corresponding author

Abstract: Aiming at the problem that the accuracy of the current compensation model for laser gyro bias error is low, an improved RBFNN bias error compensation model of laser gyro is proposed. The standardisation constant and data centre of the original data are obtained through the self-organising feature mapping network. The sample centre of the new sample data is obtained by the fastest decline of the expected variance of OLS algorithm. The results show, the improved RBF neural network algorithm has the best performance. under normal temperature, temperature change rate of 1°C/min and temperature change rate of 3°C/min, the zero-bias range of laser gyro is 3.491–3.508°C/h, 3.992–4.021°C/h and 4.092–4.123°C/h, respectively. The research results provide new reference suggestions for the zero bias temperature compensation scheme of laser gyro at different temperatures.

Keywords: laser gyroscope; radial basis function neural network; self-organising feature mapping network; least square method; temperature compensation.

Reference to this paper should be made as follows: Cui, J. and Zhong, C. (2023) 'Zero-bias error compensation method of laser gyro based on neural network', *Int. J. Wireless and Mobile Computing*, Vol. 24, No. 1, pp.91–100.

Biographical notes: Juan Cui is an Associate Professor with the Department of Basic Courses of Xi'an Traffic Engineering Institute, Xi'an, China. She received her Master's degree in Optics at Xidian University in 2010. Her research interests are inertial sensors and optoelectronics.

Cong Zhong received his Master's degree in Optics at Xidian University in 2008. His research interests include inertial sensors and optoelectronics.

1 Introduction

As a completely autonomous navigation system, chronic navigation obtains the navigation parameters such as carrier material position, speed and attitude with the help of accelerometer and gyroscope. The drift of the system mainly comes from its gyroscope. At present, higher requirements are put forward for the accuracy of gyroscope at home and abroad, which is limited by the use environment, assembly process, manufacturing, material performance and other reasons. The main solution is to optimise the accuracy of the system and calculate effective compensation through the compensation technology and data pre-processing technology of computer software (Yang et al., 2021; Cheng et al., 2021; Tao et al., 2019). Different from the traditional gyroscope, laser gyro has the advantages of large measurement range, strong impact resistance and high precision, but it still has the problem of high economic cost. At this stage, foreign research on laser gyroscopes has made outstanding achievements, and the developed lg-2728, lg-904 and other laser gyroscopes have been successfully applied to the navigation system. However, the domestic research on laser gyroscope is still in the stage of continuous exploration and learning, and there is still a large gap between the scientific research ability and the road of realising the localisation of laser gyroscope. The problems faced by the laser gyroscope at this stage are mainly reflected in the high cost caused by factors such as weight, volume and production technology (Hao et al., 2021; Tao et al., 2020; Aviev and Enin, 2018). At present, the commonly used error modelling methods of laser

gyro include time series method, wavelet network, neural network and so on. At the same time, the temperature error model in the temperature compensation method of laser gyroscope can effectively realise the real-time temperature compensation of laser gyroscope (Klimkovich, 2021; Chen, 2022; Fang et al., 2020). In view of this, a neural network oriented zero deviation compensation model of laser gyroscope is proposed and compared with the improved model, in order to improve the temperature compensation effect of laser gyroscope in China. The overall structure of the research is as follows. The second part describes the radial basis function neural network and its optimisation process. The third part introduces the laser gyro-bias error compensation model combined with the improved RBFNN. The fourth part analyses the performance and pre-processing effect of the improved RBFNN algorithm, as well as the optical gyro-bias temperature compensation results. In the fifth part, the compensation effect of laser gyro-bias error is summarised, and the shortcomings and prospects of the research are put forward.

2 Radial basis function neural network and its optimisation

2.1 Radial basis function neural network

Neural network is a mathematical algorithm model of distributed parallel information processing implemented by simulating the behaviour characteristics of animal neural network. The network plays the purpose of analysing information through the relationship between internal nodes of the system. According to the model structure, neural network can be divided into feedback network and multilayer perceptron network. The former can be regarded as a large-scale nonlinear mapping system, and the latter can be regarded as a large-scale nonlinear dynamic system. Radial Basis Function (RBF) neural network and Back Propagation (BP) neural network are the two most common neural network algorithms. The topological structures of BP neural network and RBF neural network are shown in Figure 1(a) and 1(b), respectively. The structure of BP neural network is divided into three layers: input layer, hidden layer and output layer. There is no relationship between the structures of each level. Data transmission is divided into forward propagation and back propagation. The back propagation carries out network learning by constantly modifying the weight and threshold (Klimkovich, 2021; Chen, 2022). This structure can ensure that the network can realise active learning and has the ability of nonlinear classification. The number of nodes t in the hidden layer is determined by equation (1).

$$t \geq \sqrt{x+y}+s \tag{1}$$

In equation (1), the number of nodes x and y in the input layer and the output layer is expressed respectively, s is a constant and the value range is 1–10. The transfer function of the hidden layer uses the Tansig function, and the transfer function of the output layer is the logsig function. The dimension of RBFNN input node is n, and the hidden layer uses Gaussian function for data transmission, and its calculation formula is equation (2).

$$u_i = \exp\left(-(x-M_i)^T(x-M_i)/2\delta_i^2\right) \tag{2}$$

In equation (2), $i \in (1,t)$,the vector of the input data is expressed in $x=(x_1,x_2,...,x_n)$, and the standardisation constant is δ_i, u_i refers to the output of the node of the hidden layer, with a value range of [0,1], and the central value of the Gaussian kernel function is represented by M_i. BP neural network has some disadvantages, such as weight connection, slow convergence speed, easy to fall into local minimum, unable to determine the number of nodes in the hidden layer, global approximation and so on, which are obviously improved by RBF algorithm.

Figure 1 Topology of BP neural network and RBF neural network

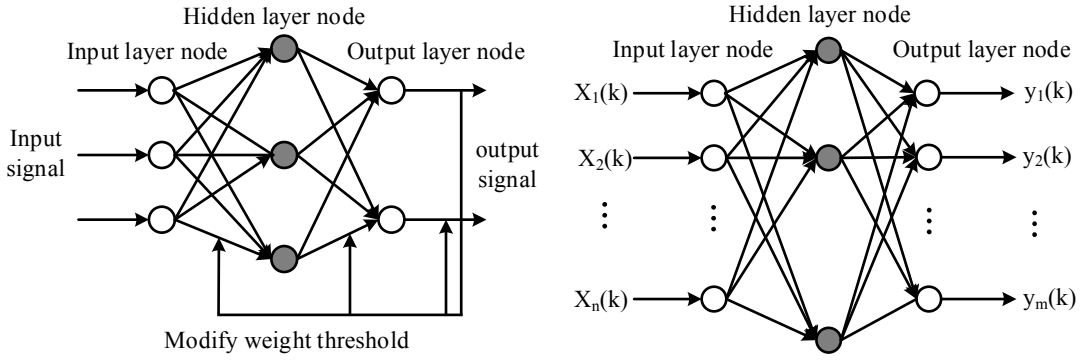

(a) Topology of BP neural network

(b) RBF neural network topology

RBF neural network is a neural network that uses the local acceptance domain to complete the function mapping based on the knowledge of overlapping acceptance region and biological local regulation. The conversion function of the hidden layer is radial basis function. Set the number of nodes in the output layer, hidden layer and input layer of RBF neural network as p,m,n, respectively. The input of RBF neural network is represented by $X=\left(x_1,x_2,...,x_j,...,x_n\right)$ and the output is represented by $Y=\left(y_1,y_2,...y_k,...,y_p\right)$. The input vector does not need to be processed by the input layer node, but is directly transmitted to the hidden layer to complete the nonlinear mapping of $X\to F_i(x)$. RBF function is a nonlinear Gaussian radial basis function, and the function is a radial symmetric function. If the distance between the data input and the symmetry centre is farther, the output of the hidden layer is smaller; On the contrary, the larger the output value of hidden layer nodes (Fang et al., 2020; Andre et al., 2019). It can be designed as any continuous value, and a basis function corresponds to each neuron. The formula of RBF function is shown in equation (3).

$$F_i(x)=\exp\left(-\left\|x-c_i\right\|/2\sigma_i^2\right),\quad i=1,2,...,m \tag{3}$$

In equation (3), the *i* perceived variable is represented by σ_i, and the value represents the width of the basis function around the centre point; The output of the i hidden layer node is represented by $F_i(x)$; n dimensional input vector is represented by *x*; The centre of the *i* basis function is denoted by c_i; The number of sensing units is represented by m. $\left\|x-c_i\right\|$ represents the distance between the two. With the increase of this value, the velocity of $F_i(x)$ decays to 0. The linear mapping $F_i(x)\to y_k$ represents the mapping from the hidden layer to the output layer. The output formula of the *k* neuron grid sequence in the output layer is equation (4).

$$\hat{y}_k=\sum_{i=1}^{m}w_{ik}F_i(x),\quad k=1,2,...,p \tag{4}$$

In equation (4), the output of the k neuron grid is denoted by $\hat{y}_k$. The number of nodes in the output layer and the hidden layer is denoted by *p* and *m* respectively, and the connection weight of the k and i neuron in the output layer and the neuron in the hidden layer is denoted by w_{ik}. The weight algorithm of RBF network is completed by single layer. Its working principle is clustering function. The clustering centre of data is obtained through training, and the sensitivity of basis function is optimised with the value of perception vector. The network in the actual working state works locally, that is, after inputting a set of data, only one neuron in the network is activated, and the activation degree of other neurons can be completely ignored (He et al., 2019; Alanis, 2018). The learning process of the network includes two aspects. First, judge the number of nodes in the hidden layer and the central value of RBF function. Secondly, the weights between the hidden layer and the output layer are continuously updated. RBF network has the following advantages: fast convergence speed, no local minimum problem, good mapping ability between output and input, full connection only between output layer and hidden layer, and linear relationship between connection weight and network output.

2.2 Optimisation of radial basis function neural network

The research selects self-organising feature mapping network (Kohonen network) to optimise RBF neural network. It is a teacher free self-organising self-learning network composed of fully interconnected neuron matrix. The optimisation idea is the response of cerebral cortex and human retina to stimulation. It is widely used in robot control, optimisation calculation, sample classification, associative storage Pattern recognition and other fields. According to the theory of self-organising feature mapping network, neurons are in different regional spaces and produce different types of division of labour. When a neural network connects the external input mode, each region will have different responses to the input mode. Neurons in the output space can form a map, in which neurons with the same function are very far away from each other, while different neurons are very far away. Since the network can complete the initial classification of samples due to its pattern classification ability, it is studied to apply it to the optimisation of RBF neural network. After completing the preliminary classification of training samples, normalisation can be completed according to the classification characteristics of different training samples, and finally the training sample set of RBF neural network is obtained (Hu et al., 2020; Jiang et al., 2018; Kohl and Miikkulainen, 2020). The self-organising feature mapping network is composed of competition layer and input layer. The connection between the two layers of neurons is two-way full connection. Self-organising feature mapping network completes the mapping through competitive learning. Competitive learning occurs in neurons at the same layer. More competitive neurons obtain and modify the connection weights connected with them, and then make the network develop in a more optimised way through competitive learning. Competitive learning is a kind of unsupervised learning. The learning process only needs to provide learning samples. The final sample output does not need to provide standard output format, but directly carries out the automatic sorting of samples and the classification of information. The classification results are expressed by the winning neurons in the competitive layer. The structure diagram of self-organising feature mapping network is shown in Figure 2. When the total input of all units in the network is calculated, the competition starts and the competition rules are set as shown in equation (5).

$$x_j^c=\begin{cases}1, S_j>\max\left(S_k,k\neq1,2,...,n\right)\\ 0,\text{others}\end{cases} \tag{5}$$

In equation (5), the output state of the j unit of the competition layer is indicated by x_j^c. After entering a mode, when the winning unit is obtained, the weight of the winning unit will be updated continuously. In this way, each time the same type of mode input is encountered, the unit of this type will have a larger input sum. The weight update rule is expressed by equation (6).

$$\Delta w_{ik} = \eta\left(\frac{x_i}{m} - w_{ik}\right) \tag{6}$$

In equation (5), the learning factor is denoted η, and the value reflects the update rate of the weight. The unit state with the input layer state of 16 is represented by m, and Δw_{ik} represents the change of weight.

Figure 2 Structure diagram of self-organising feature mapping network

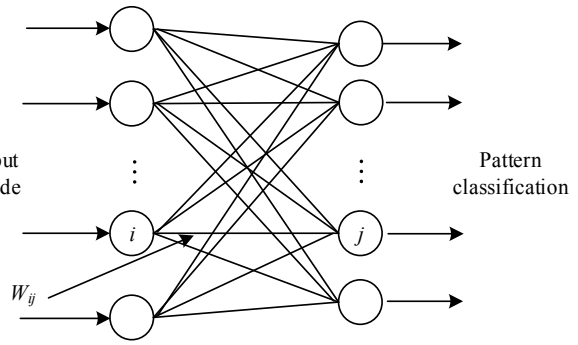

There are five common methods to determine the centre value of different RBF functions, including random selection of fixed centre, self-organising Selection Centre, supervised Selection Centre and Orthogonal Least squares (OL selection centre. Randomly selecting a fixed centre is the simplest learning strategy. In this learning strategy, only the weights need to be trained. The standard deviation and centre of the basis function are certain, and its value comes from any value in the input sample. The self-organisation selects the centre and determines the centre by clustering method, and the weight determination method is the least mean square algorithm (Eyal and Michael, 2019; Dong and Wang, 2020; Tsang et al., 2019). Supervised learning is the method of selecting the learning centre and other parameters, and the learning process is corrected by error. The orthogonal least square method takes the linear regression as a special representative, determines the number of nodes and centres and obtains the weight through the orthogonal regression matrix. OLS is selected as the selection method to optimise the radial basis function centre of RBF neural network. This method is simple to operate and requires less model conditions. At the same time, it means to ensure the minimum sum of squares of the distances from all observation points in the scatter diagram to the regression line. OLS can not only avoid the huge cost caused by the traditional random centre selection method, but also accurately and quickly identify whether the laser gyro has zero bias due to the influence of temperature.

3 Zero-bias error compensation model of laser gyro for improved RBFNN

A zero bias error compensation model of laser gyro for improved RBFNN is proposed. In the model, the RBF neural network mainly refers to the data centre of the weight, standardisation constant and radial basis function of the output node in the learning stage. The model obtains the output data of the centre of the laser gyro through the self-organising feature mapping network, and then obtains the new sample centre through the expected variance reduction of the OLS algorithm after the pre-processing method, so as to avoid the problems of numerical ill condition and large network scale. The schematic diagram of laser gyro zero-bias error compensation model for improved RBFNN is shown in Figure 3. The core of the model is to obtain the standardisation constant and data centre of the original data through the self-organising feature mapping network, and the sample centre of the new sample data through the fastest decline of the expected variance of the OLS algorithm. Specifically, firstly, the temperature data and zero bias of the laser gyro are pre-processed, and the final sample space is determined (Wang, 2018; Chaoudhary et al., 2022; Zou et al., 2021; Klimkovich, 2020). Then, the sample data are classified by self-organising feature mapping network to obtain the classification results. The learning methods of self-organising feature mapping network are as follows: firstly, randomly initialise the weights between the network learning rate and the input layer and the RBF layer. Secondly, set the network output as the dimension input vector representing the time. Thirdly, calculate the distance between each output node. Fourthly, set the node with the smallest distance as the winning output node. Fifthly, update the weight vector; Finally, when the change value of the weight value is close to or 0, the process of network learning ends (Zou et al., 2021). Then, preprocess the data obtained from the classification of self-organising feature mapping network, and obtain the data centre of improved RBF neural network through OLS algorithm (Klimkovich, 2020). The specific steps are as follows: first, select the transformation function and local perception domain of RBF neural network, set the maximum training times and allowable parameters of the network, then select the initial centre of the self-organising feature mapping network and use the transformation function to obtain the basis of the output of the hidden layer. Secondly, the training centre is obtained with the help of OLS algorithm. Finally, the training of RBF neural network is completed through the trained sample centre, and the best model is obtained.

Data pre-processing includes temperature change rate, temperature gradient and angular velocity data processing. To deal with the angular velocity, we need to subtract the angular velocity of the earth's rotation angle velocity in each channel, and then get the output data of the neural network. In view of the huge sample size of the original data, the research needs to smooth the data to avoid the cumulative effect of sample data caused by other error sources. For the treatment of temperature change rate and gradient, the final selected temperature output is the average

value of temperature sensor. The temperature change rate can be fitted by quartic polynomial. The change law of temperature, temperature gradient and temperature change rate in three directions of gyroscope is shown in Figure 4.

Figure 3 Schematic diagram of laser gyro zero-bias error compensation model for improved RBFNN

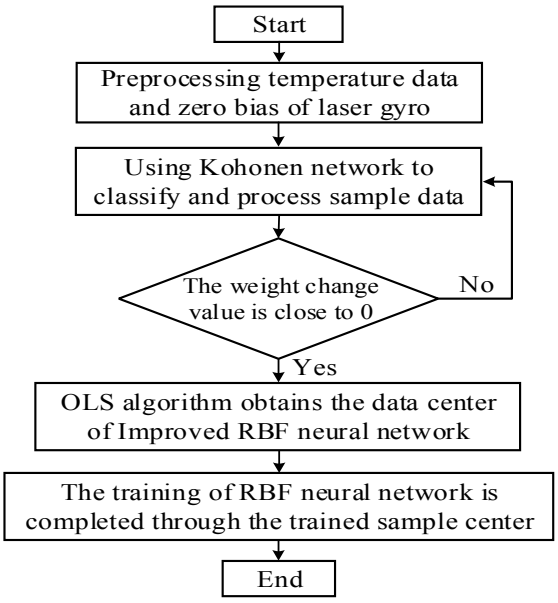

The calculation formula of the zero-bias error compensation model of laser gyro is shown in equation (7).

$$\frac{\Delta N}{\Delta t} = \left[K_0 + K_1(\Omega_I) + K_2(\Delta T) + K_3(\dot{T}) \right] \times \left[D_0 + D_1(\Delta T) + D_2(\dot{T}) + D_R + \Omega_I \right] \tag{7}$$

In equation (7), ΔN refers to the pulse given by the hall sensor to start and stop counting, Δt refers to the actual sampling period, ΔT refers to the temperature difference between the base of the laser gyro and the channel axis, $\dot{T}$ refers to the change rate of the channel axis temperature of the laser gyro, Ω_I refers to the input angular velocity, D_R refers to the random error, and D_0 refers to the zero deviation of the constant value of the gyro, The gyro-bias temperature error function is represented by D_1 and D_2. Since the variation of gyroscale factor at different temperatures is very small, there is no need to implement temperature compensation for the scale factor. The number of samples is 300 and the classification is 50. For the data acquisition of laser gyro, the research is divided into two cases: normal temperature and variable temperature. During the normal temperature experiment, first place the laser gyro in a large temperature box and keep it warm at 20°C for 2 h, then turn on the laser gyro and close the temperature box, and then record the temperature change value and zero bias of the laser gyro. The sampling period is 1 Hz and the length of the sampling data is 8 h. In the case of variable temperature, the variation range of the temperature box is – 40–60°C, set the initial temperature to 0°C, and also store it for 2 h. Set the change rate of the temperature box to 1°C / min, record the temperature change value and zero bias of the laser gyro, when the temperature increases to 60°C, do not continue to increase the temperature and keep the insulation box for 2 h; Then, use the same temperature change rate to reduce the temperature until the temperature drops to – 40°C, and keep the incubator for 2 h. Repeat the above steps to record the temperature change value and zero bias of the laser gyro. The sampling period and sampling data are the same as those of the normal temperature experiment. Then set the temperature change rate to 3°C / min, and record the temperature change value and zero bias of the laser gyro under the changing environment.

The loss of the model is calculated by three indicators: Mean Absolute Error (MAE), Root Mean Square Error (RMSE) and Mean Absolute Percentage Error (MAPE). The value range of the three indicators is any positive real-number. Mae represents the error between the real-value and the predicted value. The greater the value, the greater the difference between the error value and the real-value. RMSE refers to the deviation between the real-value and the predicted value. The greater the value, the greater the deviation between the error value and the real-value. MAPE refers to the dispersion of data. The greater the prediction accuracy of the model, the smaller the value of MAPE. The calculation formula of MSE is equation (8).

$$MSE = \frac{1}{n}\sum_{i=1}^{n}\left(U_i - \hat{U}_i\right)^2 \tag{8}$$

In equation (8), n represents the number of samples, and the training value and output value of the second sample of the neural network are represented by U_i and $\hat{U}_i$, respectively.

Figure 4 Variation law of temperature, temperature gradient and temperature change rate in three directions of gyroscope

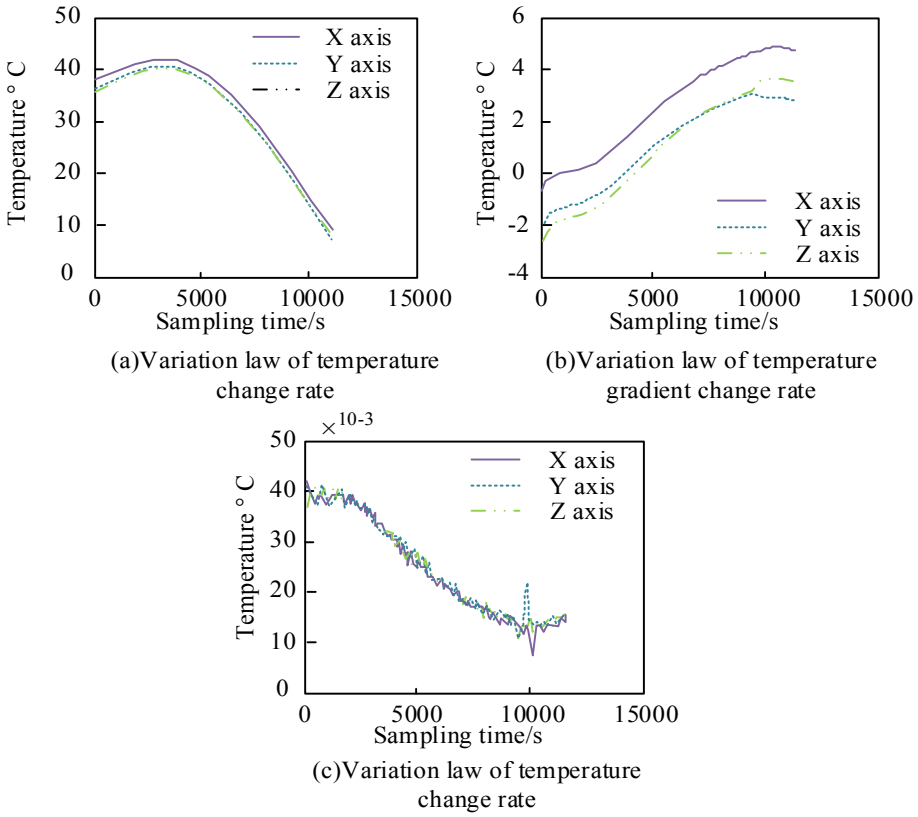

(a)Variation law of temperature change rate

(b)Variation law of temperature gradient change rate

(c)Variation law of temperature change rate

4 Analysis of compensation effect of zero bias error of laser gyro

4.1 Improve the performance and pre-processing effect of RBFNN algorithm

Firstly, the performance of the improved RBFNN algorithm is verified by MATLAB simulation platform. The learning rate is 0.5. In order to ensure the reliability of the results, the experiment was carried out 10 times and the average value was taken as the final result. The results of MAE, RMSE and MAPE errors are shown in Figures 5(a), 5(b) and 5(c). As can be seen from Figure 5(a), the MAE of five network structures such as dep belief network (DBN) decreases with the increase of iteration times, and the variation range is 8.23–426.36. The MAE of RBF neural network and BF neural network is higher than that of self-organising feature map network, improved RBF neural network and DBN. The self-organising feature map network, improved RBF neural network and DBN all converge rapidly when the number of iterations is about 20. The difference between the three algorithms is not particularly obvious. However, when the number of iterations ranges from 20 to 100, compared with self-organising feature map network and DBN, the improved RBF neural network algorithm has faster convergence speed and Mae tends to be more stable. It can be seen from Figure 5(b) that the RMSE of the five network structures decreases with the increase of the number of iterations, and the variation range is 4.16–214.21. The RMSE of RBF neural network and BF neural network is higher than that of self-organising feature map network, improved RBF neural network and DBN. The self-organising feature map network, improved RBF neural network and DBN all converge rapidly when the number of iterations is about 20. The difference between the two algorithms is not particularly obvious. As can be seen from Figure 5(c), the MAPE of the five network structures decreases with the increase of the number of iterations, ranging from 1.02 to 41.23. The self-organising feature map network, improved RBF neural network and DBN all converge rapidly when the number of iterations is about 20. The difference between the three algorithms is not particularly obvious. However, when the number of iterations ranges from 20 to 100, compared with the self-organising feature map network algorithm and DBN, the improved RBF neural network algorithm has faster convergence speed and MAPE tends to be more stable.

The zero-bias data of laser gyro collected in three cases are smoothed for 100 seconds, and the results are shown in Figures 6(a), 6(b) and 6(c). On the whole, the zero bias of laser gyroscope is very stable at room temperature, but with the increase of temperature change rate, the zero bias of laser gyroscope will be seriously affected by temperature. Under normal temperature, the zero-bias range of laser gyro is 3.491–3.508°C / h; When the temperature change rate is 1°C / min, the zero-bias range of the laser gyro is 3.992–4.021°C / h, this is because with the increase of temperature change rate, the adaptability of the laser gyroscope will be reduced, resulting in a large zero bias range of the laser gyroscope; When the temperature change rate is 3°C / min, the zero-bias range of the laser gyro is 4.092–4.123°C / h. Therefore, the zero-bias temperature compensation of laser gyro is of great significance when the temperature change rate is large.

Figure 5 Training loss results of five neural networks

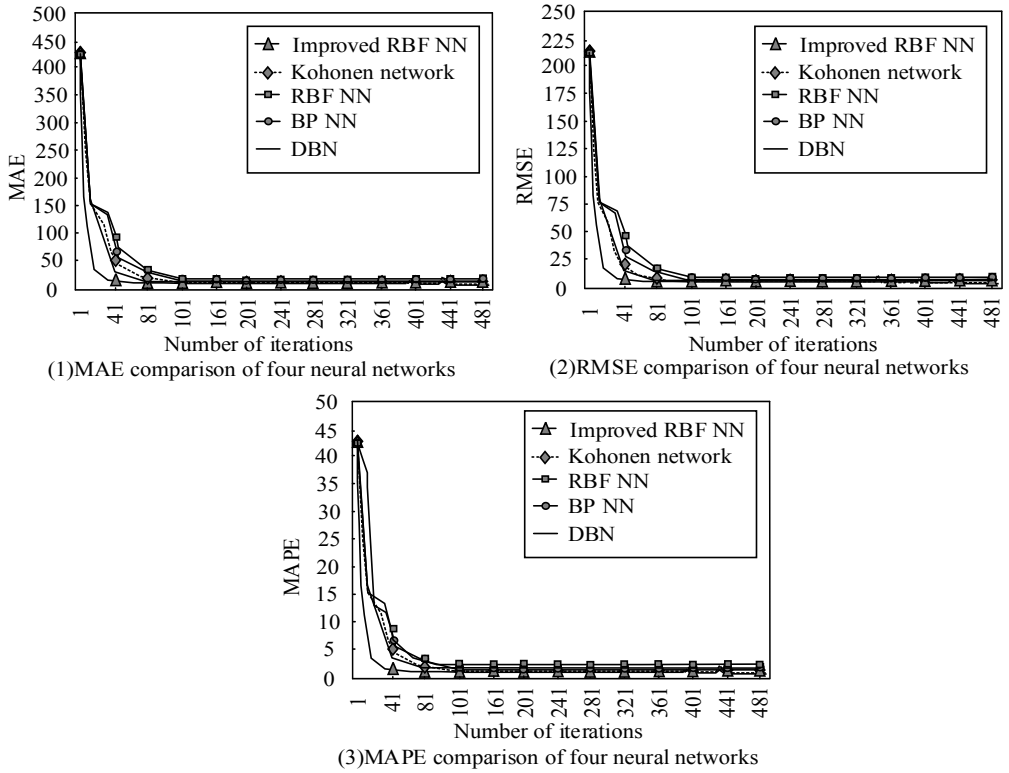

(1)MAE comparison of four neural networks

(2)RMSE comparison of four neural networks

(3)MAPE comparison of four neural networks

Figure 6 Smoothing results of laser gyro zero-bias data in three cases

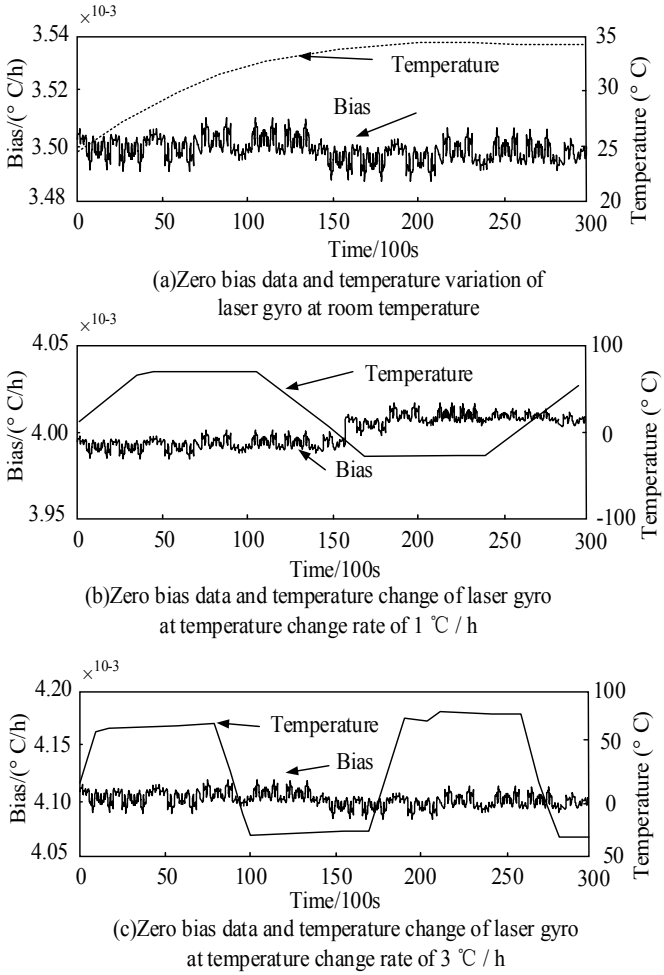

(a)Zero bias data and temperature variation of laser gyro at room temperature

(b)Zero bias data and temperature change of laser gyro at temperature change rate of 1 ℃ / h

(c)Zero bias data and temperature change of laser gyro at temperature change rate of 3 ℃ / h

4.2 Analysis of zero bias temperature compensation results of laser gyro

The output of RLG of RBF neural network at three different temperatures is shown in Figures 7(a), 7(b) and 7(c). Under normal temperature, the zero-bias range of the laser gyro under the network is 3.493–3.512°C / h; When the temperature change rate is 1°C / min, the zero-bias range of the laser gyro is 3.993–4.023°C / h; When the temperature change rate is 3°C / min, the zero-bias range of the laser gyro is 4.098–4.131°C / h. It can be seen that the network can better fit the influence of temperature in the bias of laser gyro.

Figure 7 Llaser gyro output of RBF neural network at three different temperatures

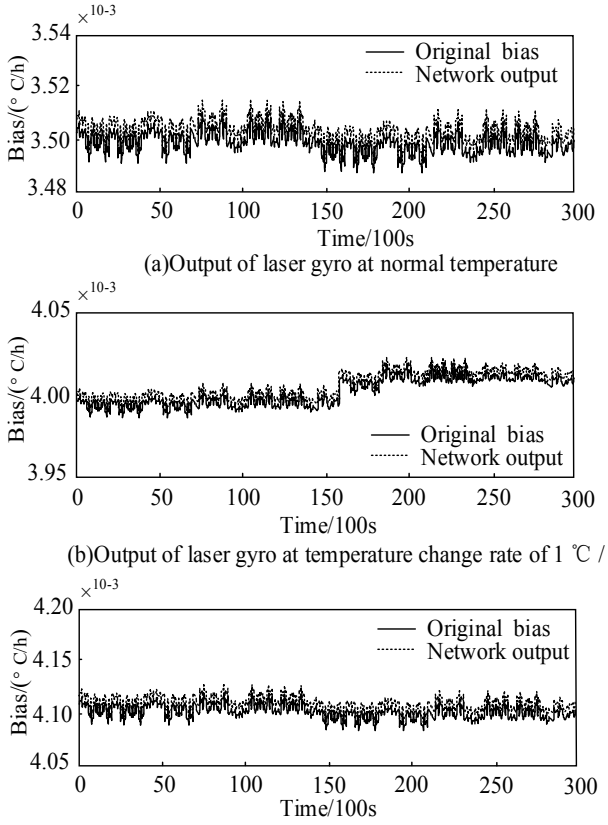

(a)Output of laser gyro at normal temperature

(b)Output of laser gyro at temperature change rate of 1 ℃ / h

(c)Output of laser gyro at temperature change rate of 3 ℃ / h

The output of RLG with improved RBF neural network at three different temperatures is shown in Figures 8(a), 8(b) and 8(c). Under normal temperature, the zero-bias range of laser gyro is 3.492–3.509°C / h; When the temperature change rate is 1°C / min, the zero-bias range of the laser gyro is 3.991–4.020°C / h; When the temperature change rate is 3°C / min, the zero-bias range of the laser gyro is 4.091–4.122°C / h. Compared with the output of RLG based on RBF neural network, it can be seen that the network can better fit the influence of temperature in RLG bias.

The zero-bias temperature compensation results of RLG based on RBF neural network at three different temperatures are shown in Figures 9(a), 9(b) and 9(c). After compensation, the zero bias of the laser gyro will not be affected by temperature. Under normal temperature, the zero-bias range of laser gyro is –0.0012–0.0008°C / h; When the temperature change rate is 1°C / min, the zero-bias range of the laser gyro is –0.0009–0.0008°C / h; When the temperature change rate is 3°C / min, the zero-bias range of the laser gyro is –0.0009–0.0008°C / h. The temperature compensation accuracy under normal temperature, temperature change rate of 1°C / min and temperature change rate of 3°C / min is 99.1%, 98.9% and 98.8%, respectively, which does not meet the requirements of temperature compensation accuracy.

Figure 8 Laser gyro output of Improved RBF neural network at three different temperatures

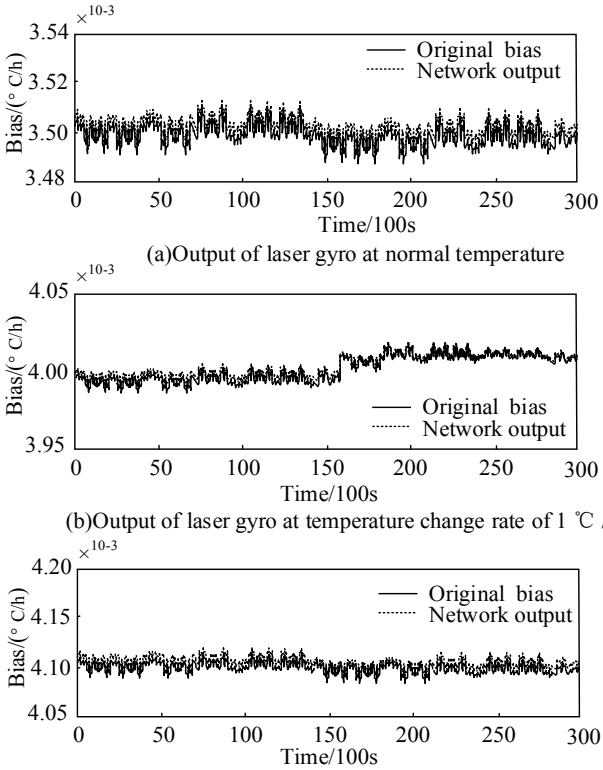

(a)Output of laser gyro at normal temperature

(b)Output of laser gyro at temperature change rate of 1 ℃ / h

(c)Output of laser gyro at temperature change rate of 3 ℃ / h

The zero-bias temperature compensation results of laser gyro based on Improved RBF neural network under three different temperatures are shown in Figures 10(a), 10(b) and 10(c), respectively. After compensation, the zero bias of the laser gyro will not be affected by temperature. Under normal temperature, the zero-bias range of laser gyro is –0.0012–0.0008°C / h; When the temperature change rate is 1°C / min, the zero-bias range of the laser gyro is –0.0009–0.0008°C / h; When the temperature change rate is 3°C / min, the zero-bias range of the laser gyro is –0.0009–0.0008°C / h. The temperature compensation accuracy under normal temperature, temperature change rate of 1°C / min and temperature change rate of 3°C / min are 99.6%, 99.7% and 99.8%, respectively, meeting the requirements of temperature compensation accuracy. At the same time, in terms of time-consuming, the time spent by the improved RBF neural network is less than 90 s, while the time spent by the non-optimised RBF neural network is more than 130 s, which shows that the time spent by the improved RBF neural network is significantly less than that of the non-optimised RBF neural network. The temperature compensation efficiency is greatly improved.

Figure 9 Zero-bias temperature compensation results of laser gyro based on RBF neural network at three different temperatures

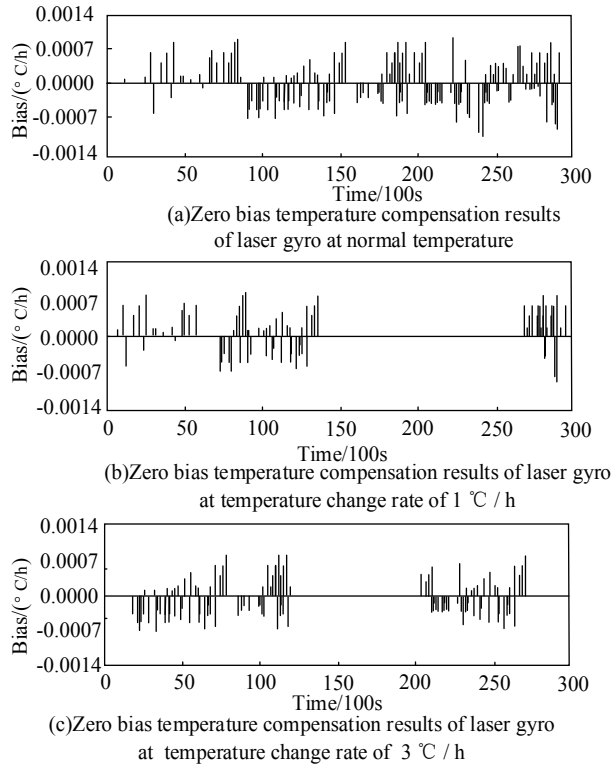

(a)Zero bias temperature compensation results of laser gyro at normal temperature

(b)Zero bias temperature compensation results of laser gyro at temperature change rate of 1 ℃ / h

(c)Zero bias temperature compensation results of laser gyro at temperature change rate of 3 ℃ / h

Figure 10 Zero-bias temperature compensation results of laser gyro based on improved RBF neural network at three different temperatures

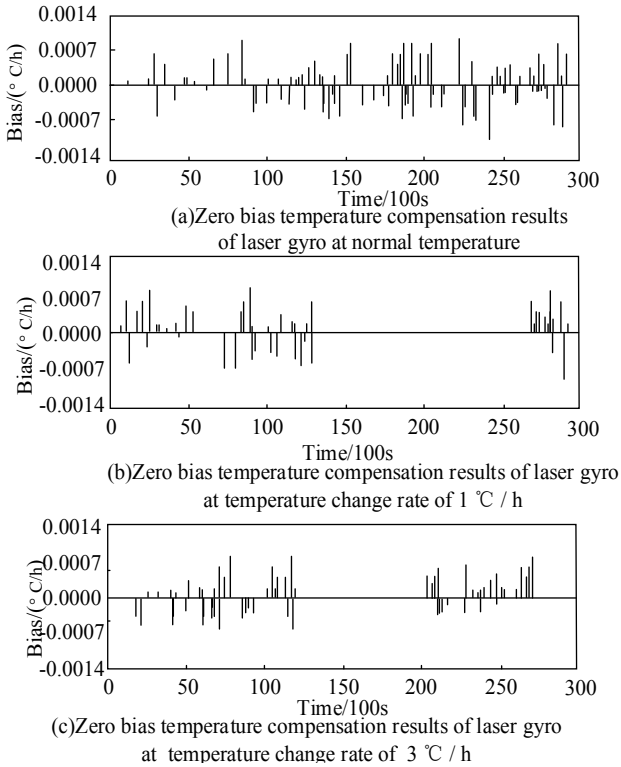

(a)Zero bias temperature compensation results of laser gyro at normal temperature

(b)Zero bias temperature compensation results of laser gyro at temperature change rate of 1 ℃ / h

(c)Zero bias temperature compensation results of laser gyro at temperature change rate of 3 ℃ / h

5 Conclusions

The zero-bias temperature compensation of laser gyro has always been a topic of close attention by experts and scholars at home and abroad. Aiming at the problems of low precision and poor stability of laser gyro in China, a neural network-oriented compensation model for laser gyro-bias temperature error is proposed, which can effectively compensate the influence of temperature on laser gyro-bias error. Firstly, the principle and defects of RBF network algorithm are proposed, and then the RBF neural network is optimised by OLS algorithm and self-organising feature mapping network. Secondly, the original laser gyro-bias data is pre-processed. Finally, the performance of zero-bias temperature compensation method is verified and compared by setting temperature compensation experiments at three temperatures. The results of neural network performance test show that with the increase of iteration times, the MAE, RMSE and MAPE of the five network structures gradually decrease, and the variation ranges of the three errors are 8.23–426.36, 4.16–214.21 and 1.02–41.23, respectively. Under normal temperature, the zero-bias range of laser gyro is 3.491–3.508°C / h; When the temperature change rate is 1°C / min, the zero-bias range of the laser gyro is 3.992–4.021°C / h; When the temperature change rate is 3°C / min, the zero bias range of the laser gyro is 4.092–4.123°C / h. The time consumed by the improved RBF neural network is also less than 90 s, which is significantly less than that of the non-optimised RBF neural network. Therefore, the improved RBF neural network can not only greatly improve the temperature compensation efficiency of laser gyro bias, but also greatly shorten the temperature compensation time of laser gyro bias. Limited by our time and energy, the dispersion constant of RBF network has not been determined in the research, and the proposed neural network optimisation algorithm has not been applied in practice. Subsequent optimisation and improvement are needed to improve the practical value of the research.

References

Alanis, A.Y. (2018) 'Electricity prices forecasting using artificial neural networks', *International Journal of IEEE Latin America Transactions*, Vol. 16, No. 1, pp.105–111.

Andre, E., Brett, K. and Novoa, R.A. et al. (2019) 'Dermatologist level classification of skin cancer with deep neural networks', *International Journal of Nature*, Vol. 524, No. 7639, pp.115–118.

Aviev, A.A. and Enin, V.N. (2018) 'Optical field amplitude distribution on the pattern plate of optoelectronic system for measuring of dither system parameters in ring laser gyro', *International Journal of Scientific and Technical Journal of Information Technologies Mechanics and Optics*, Vol. 18, No. 2, pp.197–204.

Chaoudhary, S., Dewasi, A. and Ram, P.S. et al. (2022) 'Laser ablation fabrication of a p-NiO/n-Si heterojunction for broadband and self-powered UV-Visible-NIR photodetection', *International Journal of Nanotechnology*, Vol. 33, No. 25, pp.255202–255215.

Chen, Z. (2022) 'Research on internet security situation awareness prediction technology based on improved RBF neural network algorithm', *Journal of Computational and Cognitive Engineering*. Doi: 10.47852/bonviewJCCE149145205514.

Cheng, G., Zhang, Y. and Lei, H. et al. (2021) 'The application of the vibration absorber in laser inertial navigation products ', *International Journal of Sensors*, No. 6, pp.1–7.

Dong, Y. and Wang, H. (2020) 'Robust output feedback stabilization for uncertain discrete-time stochastic neural networks with time-varying delay', *International Journal of Neural Processing Letters*, Vol. 51, No. 1, pp.83–103.

Eyal, K. and Michael, M. (2019) 'Knowledge extraction from neural networks using the all-permutations fuzzy rule base: the LED display recognition problem', *International Journal of IEEE Transactions on Neural Networks*, Vol. 18, No. 3, pp.925–956.

Fang, F., Zeng, W. and Li, Z. (2020) 'Coupled dynamic analysis and decoupling optimization method of the laser gyro inertial measurement unit', *International Journal of Sensors (Basel, Switzerland)*, Vol. 20, No. 1, pp.111–134.

Hao, D., Tang X. and An, Y. et al. (2021) 'Orientation switching of single molecules on surface excited by tunneling electrons and ultrafast laser pulses ', *International Journal of Physical Chemistry Letters*, Vol. 12, No. 7, pp.2011–2016.

He, H., Gang, F. and Jinde, C. (2019) 'Robust state estimation for uncertain neural networks with time-varying delay', *International Journal of Jishou University(Natural Sciences Edition)*, Vol. 19, No. 8, pp.1329–1339.

Hu, J., Hua, F. and Tian, W. (2020) 'Robot positioning error compensation method based on deep neural network ', *International Journal of Physics Conference Series*, Vol. 1487, pp.012045–012054.

Jiang, Y.G., Wu, Z. and Wang, J. et al.(2018) 'Exploiting feature and class relationships in video categorization with regularized deep neural networks', *International Journal of IEEE Transactions on Pattern Analysis and Machine Intelligence*, Vol. 40, No. 2 , pp.352–364.

Klimkovich, B.V. (2020) 'Influence of random error of temperature sensors on the quality of temperature compensation of fog bias by the neural network', *International Journal of Giroskopiya i Navigatsiya*, Vol. 28, No. 4, pp.53–70.

Klimkovich, B.V. (2021) 'Effect of random error of temperature sensors on the quality of temperature compensation of FOG bias by a neural network', *International Journal of Gyroscopy and Navigation*, Vol. 12, No. 1, pp.27–37.

Kohl, N. and Miikkulainen, R. (2020) 'Evolving neural networks for strategic decision-making problems', *International Journal of Annals of Surgical Oncology*, Vol. 22, No. 3, pp.326–337.

Tao, Y., Li, S. and Fu, Q. et al. (2020) 'A method for improving light intensity stability of a total reflection prism laser gyro based on series correction and feedforward compensation', *International Journal of IEEE Access*, Vol. 8, No. 99, pp.13651–13660.

Tao, Y., Li, S. and Zheng, J. et al. (2019) ' High precision compensation for a total reflection prism laser gyro bias in consideration of high frequency oscillator voltage', *International Journal of Sensors (Basel, Switzerland)*, Vol. 19, No. 13, pp.2986–3002.

Tsang, E., Yeung, D.S. and Lee, J. et al. (2019) 'Refinement of generated fuzzy production rules by using a fuzzy neural network', *International Journal of JIEEE Transactions on Systems, Man, and Cybernetics. Part B, Cybernetics: a Publication of the IEEE Systems, Man, and Cybernetics Society.*, Vol. 34, No. 1, pp.409–427.

Wang, J. (2018) 'Research on zero speed correction of laser gyro strapdown inertial navigation system', *International Journal of Yadian Yu Shengguang/Piezoelectrics and Acoustooptics*, Vol. 40, No. 4, pp.626–632.

Yang, C., Cai, Y. and Xin, C. et al. (2021) 'Research on temperature error compensation method of vehicle-mounted laser gyro SINS', *International Journal of Physics: Conference Series*, Vol. 1885, No. 4, pp.042020–042027.

Zou, D., Thirkettle, R.J. and Gebauer, A. et al. (2021) 'Gyroscopic performance and some seismic measurements made with a 10 metre perimeterring laser gyro housed in the Ernest Rutherford Building', *International Journal of Applied Optics*, Vol. 60, No.6 , pp.1737–1743.